

# A Hybrid AC/DC Micro grid With Fuzzy Logic Controller

Ganesula Prasad, Shaik Dawood

**Abstract**— The proposed system presents power- control strategies of a grid-connected Micro grid generation system with versatile power transfer. This Micro grid system allows maximum utilization of freely available renewable energy sources like wind and photovoltaic energies. For this, an adaptive MPPT P&O Controller along with standard perturb and observes method will be used for the system.

The proposed Micro grid can operate in autonomous mode. fuzzy logic controller and controlling converters are proposed for smooth power transfer between ac and dc links and for stable system operation under various generation and load conditions. This Micro grid system operates under normal conditions which include normal room temperature in the case of solar energy and normal wind speed at plain area in the case of wind energy. The Power Balancing Control simulation results are presented to illustrate the operating principle, feasibility and reliability of Micro grid proposed system

**Index Terms**— Hybrid microgrid, PV system, Wind power generation, Fuzzy logic controller.

## I. INTRODUCTION

Even though three phase ac power systems have existed for over 100 years due to their efficient transformation of ac power at different voltage levels, keeping in mind the environmental issues such as global warming, pollution, depletion of fossil fuels time had come to concentrate on renewable sources of energy. More and more dc loads such as light-emitting diode (LED) lights and electric vehicles (EVs) are connected to ac power systems to save energy and reduce CO<sub>2</sub> emission. When power can be fully supplied by local renewable power sources, long distance high voltage transmission is no longer necessary. A hybrid AC/DC micro grid [1] have been proposed to facilitate the connection of renewable power sources to conventional ac systems. However, dc power from the renewable photovoltaic (PV) panels or fuel cells has to be converted into ac using dc/dc boosters and dc/ac inverters in order to connect to an ac grid. In an ac grid, embedded ac/dc and dc/dc converters are required for various home and office facilities to supply different dc voltages. AC/DC/AC converters are commonly used as drives in order to control the speed of ac motors in industrial plants. A hybrid ac/dc microgrid is proposed in this paper to reduce the processes of multiple reverse conversions in an individual ac or dc grid and to facilitate the connection of various renewable ac and dc sources and loads to power

system. Since energy management, control, and operation of a hybrid grid are more complicated than those of an individual ac or dc grid, different operating modes of a hybrid ac/dc grid have been investigated. The coordination control schemes among various converter have been proposed to harness maximum power from renewable power sources, to minimize power transfer between ac and dc networks, and to maintain the stable operation of both ac and dc grids under variable supply and demand conditions when the hybrid grid operates in both grid-tied and islanding modes.

## II. SYSTEM CONFIGURATION AND MODELING

### A. Grid Configuration

Fig.1 shows a conceptual hybrid system where various ac and dc sources and loads are connected to the corresponding dc and ac networks. The ac and dc links are connected together through two transformers and two four- quadrant operating three phase converters. The ac bus of the hybrid grid is tied to the utility grid. A compact hybrid grid as shown in Fig.2 is modeled using the Simulink in the MATLAB to simulate system operations and controls. Forty kW PV arrays are connected to dc bus through a dc/dc boost converter to simulate dc sources. A capacitor  $C_{pv}$  is to suppress high frequency ripples of the PV output voltage. A 50 kW wind turbine generator (WTG) with doubly fed induction generator (DFIG) is connected to an ac bus to simulate ac sources. A 65 Ah battery as energy storage is connected to dc bus through a bidirectional dc/dc converter. Variable dc load (20 kW–40 kW) and ac load (20 kW–40 kW) are connected to dc and ac buses respectively. The rated voltages for dc and ac buses are 400V and 400V rms respectively. A three phase bidirectional dc/ac main converter with R-L-C filter connects the dc bus to the ac bus through an isolation transformer

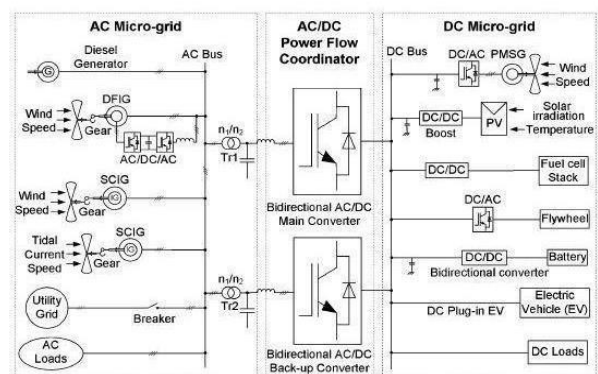


Fig. 1. A Hybrid AC/DC microgrid system

### B. Grid Operation

The hybrid grid can operate in two modes. In grid-tied mode, the main converter is to provide stable dc bus voltage and required reactive power and to exchange power between the ac and dc buses. The boost converter and WTG are controlled to provide the maximum power. When the output power of the dc sources is greater than the dc loads, the converter acts as an

Manuscript received March 03, 2016

Ganesula Prasad, M.tech Student, EEE department, Nimra Institute Of Science & Technology

Shaik Dawood, Assistant professor, EEE department, Nimra Institute Of Science & Technology

inverter and injects power from dc to ac side. When the total power generation is less than the total load at the dc side, the converter injects power from the ac to dc side. When the total power generation is greater than the total load in the hybrid grid, it will inject power to the utility grid.

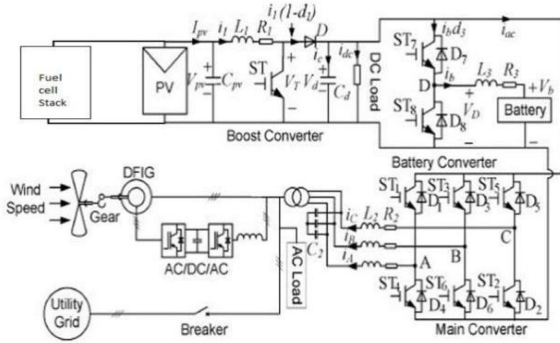


Fig. 2. A compact representation of the proposed Hybrid grid

Otherwise, the hybrid grid will receive power from the utility grid. In the grid tied mode, the battery converter is not very important in system operation because power is balanced by the utility grid. In autonomous mode, the battery plays a very important role for both power balance and voltage stability. Control objectives for various converters are dispatched by energy management system. DC bus voltage is maintained stable by a battery converter or boost converter according to different operating conditions. The main converter is controlled to provide a stable and high quality ac bus voltage. Both PV and WTG can operate on maximum power point tracking (MPPT) or off-MPPT mode based on system operating requirements. Variable wind speed and solar irradiation are applied to the WTG and PV arrays respectively to simulate variation of power of ac and dc sources and test the MPPT control algorithm.

**C. Modeling of PV Panel**

Fig. 3 shows the equivalent circuit of a PV panel with a load. The current output of the PV panel is modeled by the following three equations [1].

$$I_{pv} = I_{ph} - I_s [\exp(q(V_{pv} + I_{pv} R_s) / KTC) - 1] - (V_{pv} + I_{pv} R_s) / R_p \dots \dots \dots (1)$$

$$I_{ph} = [I_{sc} + K_1(TC - T_{REF}) \lambda] / 1000 \dots \dots \dots (2)$$

$$I_s = I_{rs} [TC / T_{REF}]^3 \exp [q E_G (1 / T_{REF} - 1 / TC) / kA] \dots \dots \dots (3)$$

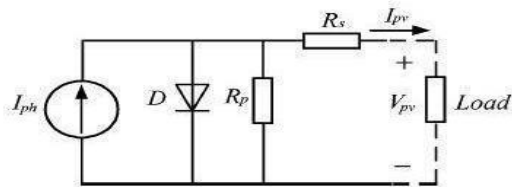


Fig.3. Equivalent circuit of a solar cell.

**D. Modeling of Battery**

Two important parameters to represent state of a battery are terminal voltage  $V_b$  and state of charge (SOC) as follows [1]

$$V_b = V_0 + R_b I_b - k (Q / Q - \int I_b . dt) + A \cdot \exp(B \int I_b . dt) \quad (4)$$

$$SOC = 100(1 + (\int I_b . dt) / Q) \quad (5)$$

where  $R_b$  is internal resistance of the battery,  $V_0$  is the open circuit voltage of the battery,  $\int I_b . dt$  is battery charging

current, is polarization voltage, is battery capacity, is exponential voltage, and is exponential capacity

**E. Modeling of Wind Generator**

Power output  $P_m$  from a WTG is determined by

$$P_m = (1/2)(\rho A (V\omega)^3) C_p(\lambda, \beta) \quad (6)$$

Where  $\rho$  is air density,  $A$  is rotor swept area,  $V\omega$  is wind speed, and  $C_p(\lambda, \beta)$  is the power coefficient, which is the function of tip speed ratio  $\lambda$  and pitch angle  $\beta$ .

The mathematical models of a DFIG are essential requirements for its control system. The voltage equations of an induction motor in a rotating d-q coordinate are as follows:

$$\begin{bmatrix} U_{ds} \\ U_{qs} \\ U_{dr} \\ U_{qr} \end{bmatrix} = \begin{bmatrix} -R_s & 0 & 0 & 0 \\ 0 & -R_s & 0 & 0 \\ 0 & 0 & R_r & 0 \\ 0 & 0 & 0 & R_r \end{bmatrix} \begin{bmatrix} i_{ds} \\ i_{qs} \\ i_{dr} \\ i_{qr} \end{bmatrix} + P \begin{bmatrix} \lambda_{ds} \\ \lambda_{qs} \\ \lambda_{dr} \\ \lambda_{qr} \end{bmatrix} + \begin{bmatrix} -w_1 \lambda_{qs} \\ w_1 \lambda_{ds} \\ -w_2 \lambda_{qr} \\ w_2 \lambda_{dr} \end{bmatrix}$$

$$\begin{bmatrix} \lambda_{ds} \\ \lambda_{qs} \\ \lambda_{dr} \\ \lambda_{qr} \end{bmatrix} = \begin{bmatrix} -L_s & 0 & -L_m & 0 \\ 0 & -L_s & 0 & -L_m \\ -L_m & 0 & L_r & 0 \\ 0 & -L_m & 0 & L_r \end{bmatrix} \begin{bmatrix} i_{ds} \\ i_{qs} \\ i_{dr} \\ i_{qr} \end{bmatrix}$$

The dynamic equation of the DFIG

$$(J / np) d/dt(\omega_r) = T_m - T_{em} \quad (7)$$

$$T_e = np L_m (I_{qs} I_{dr} - I_{ds} I_{qr}) \quad (8)$$

where the subscripts d, q, s, and r denote d-axis, q-axis,

stator and rotor respectively,  $L$  represents the inductance,  $\lambda$  is the flux linkage and  $u$  and  $I$  represent voltage and current respectively, and  $\omega_1$  and  $\omega_2$  are the angular synchronous speed and slip speed respectively,  $\omega_2 = \omega_1 - \omega_r$ ,  $T_m$  is the mechanical torque,  $T_{em}$  is the electromagnetic torque.

If the synchronous rotating  $d-q$  reference is oriented by the stator voltage vector, the  $d$ -axis is aligned with the stator voltage vector while the  $q$ -axis is aligned with the stator flux reference frame. Therefore,  $\lambda_{ds} = 0$  and  $\lambda_{qs} = \lambda_s$ . The following equations can be obtained in the stator voltage oriented reference frame as [8]:

$$I_{ds} = -(L_m / L_s) I_{dr} \quad (9)$$

$$T_{em} = np (L_m / L_s) I_{dr} \lambda_{dr} \quad (10)$$

$$V_{dr} = V_{dr} + R_r I_{dr} - (\omega - \omega_r) (I_{qr} L_r + L_m I_{qs}) \quad (11)$$

$$V_{qr} = V_{qr} + R_r I_{qr} - (\omega - \omega_r) (I_{dr} L_r + L_m I_{ds}) \quad (12)$$

**F. Fuzzy Logic Controller**

the disadvantage of PI controller is its inability to react to abrupt changes in the error signal,  $\epsilon$ , because it is only capable of determining the instantaneous value of the error signal without considering the change of the rise and fall of the error, which in mathematical terms is the derivative of the error denoted as  $\Delta\epsilon$ . To solve this problem Fuzzy logic control [21] as it is shown in Fig 4 is proposed.

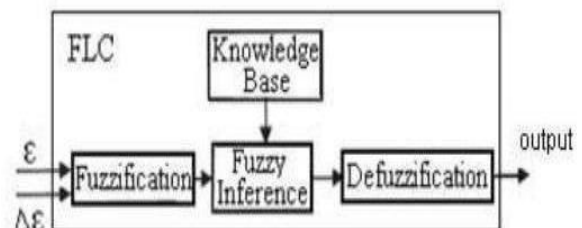


Fig.4. Basic representation of FLC

The determination of the output control signal, is done in an inference engine with a rule base having if-then rules in the form of "IF  $\varepsilon$  is ..... AND  $\Delta\varepsilon$  is ....., THEN output is."

With the rule base, the value of the output is changed

according to the value of the error signal  $\varepsilon$ , and the rate-of-error  $\varepsilon$ . The structure and determination of the rule base is done using trial-and-error methods and is also done through experimentation.

T\* All the variables' fuzzy subsets for the inputs  $\varepsilon$  and  $\Delta\varepsilon$  are defined as (NB, NM, NS, Z, PS, PM, PB) . The membership function of inputs are decided according to the system requirement.

### III. COORDINATION CONTROL OF THE CONVERTERS

There are five types of converters in the hybrid grid. Those converters have to be coordinately controlled with the utility grid to supply an uninterrupted, high efficiency, and high quality power to variable dc and ac loads under variable solar irradiation and wind speed when the hybrid grid operates in both isolated and grid tied modes. The control algorithms for those converters are presented in this section.

#### A. Grid-Connected Mode

When the hybrid grid operates in this mode, the control objective of the boost converter is to track the MPPT of the PV array by regulating its terminal voltage. The back-to-back ac/dc/ac converter of the DFIG is controlled to regulate rotor side current to achieve MPPT and to synchronize with ac grid. The energy surplus of the hybrid grid can be sent to the utility system. The role of the battery as the energy storage becomes less important because the power is balanced by the utility grid. In this case, the only function of the battery is to eliminate frequent power transfer between the dc and ac link. The main converter is designed to operate bi - directionally to incorporate complementary characteristic of wind and solar sources [10], [11]. The control objectives of the main converter are to maintain a stable dc-link voltage for variable dc load and to synchronize with the ac link and utility system.

Power flow equations at the dc and ac links are as follows:

$$P_{pv} + P_{ac} = P_{dcl} + P_b \quad (11)$$

$$P_s = P_w - P_{acl} - P_{ac} \quad (12)$$

where real power  $P_{pv}$  and  $P_w$  are produced by PV and WTG respectively,  $P_{acL}$  and  $P_{dcL}$  are real power loads connected to ac and dc buses respectively,  $P_{ac}$  is the power exchange between ac and dc links,  $P_b$  is power injection to battery, and  $P_s$  is power injection from the hybrid grid to the utility. The reference value of the solar panel terminal voltage  $V^*$  is determined by the basic perturbation and observation (P&O) algorithm based on solar irradiation and temperature to harness the maximum power [13].

To smoothly exchange power between dc and ac grids and supply a given reactive power to the ac link, PQ control is implemented using a current controlled voltage source for the main converter. Two PI controllers are used for real and

reactive power control respectively. When resource conditions or load capacities change, the dc bus voltage is adjusted to constant through PI regulation. When a sudden dc load drop causes power surplus at dc side, the main converter is controlled to transfer power from the dc to the ac side.

The DFIG is controlled to maintain a stable dc-link voltage of the back-to-back ac/dc/ac converter. The objectives of the rotor side converter are to track MPPT of the WTG and to manage the stator side reactive power. Different control schemes such as the direct torque control (DTC) and direct power control (DPC) have been proposed for a DFIG in literature [8].

The rotor rotational speed is obtained through the MPPT algorithm, which is based on the power and speed

characteristic of the wind turbine. The rotational speed  $\omega_r$  and mechanical power  $P_m^*$  are used to calculate the electromagnetic torque  $T$  The  $d$ -axis rotor side current reference is determined based on  $\omega_r$  through stator flux estimation.

#### B. Isolated Mode

When the hybrid grid operates in the islanding mode, the boost converter and the back-to-back ac/dc/ac converter of the DFIG may operate in the on-MPPT or off-MPPT based on system power balance and energy constraints. The main converter acts as a voltage source to provide a stable voltage and frequency for the ac grid and operates either in inverter or converter mode for the smooth power exchange between ac and dc links. The battery converter operates either in charging or discharging mode based on power balance in the system. The dc-link voltage is maintained by either the battery or the boost converter based on system operating condition. Powers under various load and supply conditions should be balanced as follows: Where  $P_{loss}$  is the total grid loss.

### IV. SIMULATION RESULTS

The operations of the hybrid grid under various source and load conditions are simulated to verify the proposed control algorithms.

#### A. Grid-Connected Mode

In this mode, the main converter operates in the PQ mode. Power is balanced by the utility grid. The battery is fully charged and operates in the rest mode in the simulation. AC bus voltage is maintained by the utility grid and dc bus voltage is maintained by the main converter.

The optimal terminal voltage is determined using the basic P&O algorithm based on the corresponding solar irradiation. Fig. 5 shows the curves of the solar radiation and the output power of the PV panel. The output power varies from 13.5 kW to 37.5 kW, which closely follows the solar irradiation when the ambient temperature is fixed

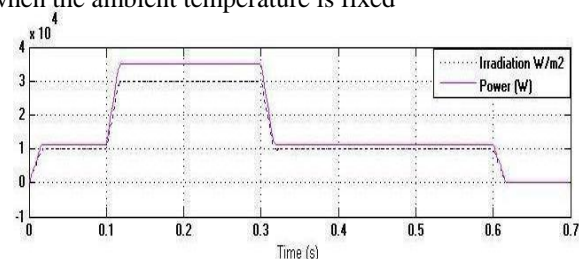


Fig.5. PV output power versus solar irradiation

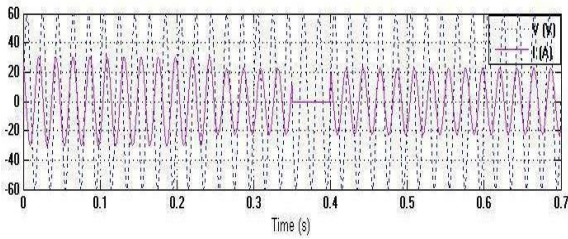


Fig. 6. AC side voltage and current of the main converter with variable solar irradiation level and constant dc load.(with PI controller)

Fig.6 shows the voltage and current responses at the ac side of the main converter when the solar irradiation level

decreases from 1000W/m<sup>2</sup> at 0.3 s to 400W/m<sup>2</sup> at 0.4 s with a fixed dc load 20 kW. It can be seen from the current directions that the power is injected from the dc to the ac grid before 0.3 s and reversed after 0.4 s

Fig.7 shows the voltage and current responses at the ac side of the main converter when the dc load increases from 20 kW to 40 kW at 0.25 s with a fixed irradiation level 750W/m<sup>2</sup>

It can be seen from the current direction that power is injected from dc to ac grid before 0.25s and reversed after 0.25 s.

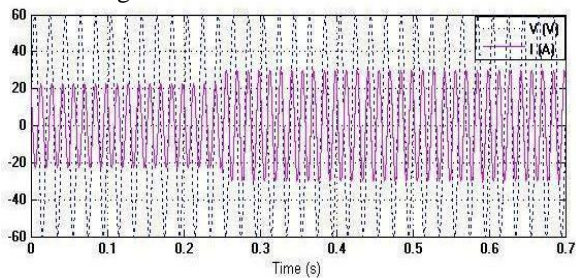


Fig. 7. AC side voltage and current of the main converter with constant solar irradiation level and variable dc load.

Fig.8 shows the voltage response at dc side of the main converter under the same conditions. The figure shows that the voltage drops at 0.25 s and recovers quickly by the controller.

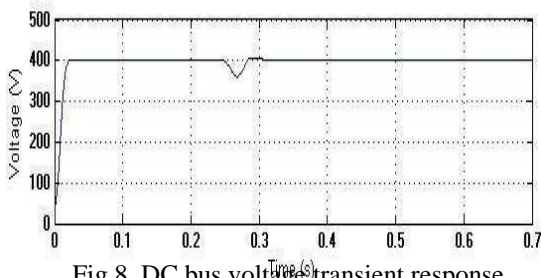


Fig.8. DC bus voltage transient response.

**B. Isolated Model**

The control strategies for the two cases i.e., on-MPPT and for off-MPPT mode are verified. In on-MPPT, dc bus voltage is maintained stable by the battery converter and ac bus voltage is provided by the main converter. The reference of dc-link voltage is set as 400V. Fig. 9 shows the transient process of the DFIG power output, which becomes stable after 0.45 s due to the mechanical inertia.

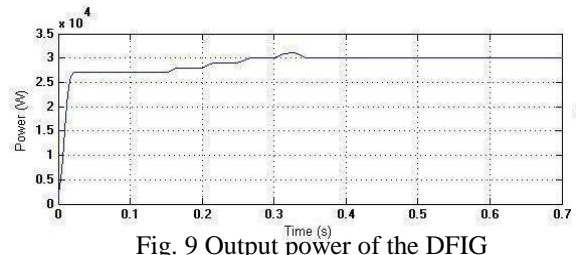


Fig. 9 Output power of the DFIG

Fig. 10 shows the dynamic responses at the ac side of the main converter when the ac load increases from 20 kW to 40kW at 0.3 s with a fixed wind speed 12 m/s. It is shown clearly that the ac grid injects power to the dc grid before 0.3 s and receives power from the dc grid after 0.3 s.

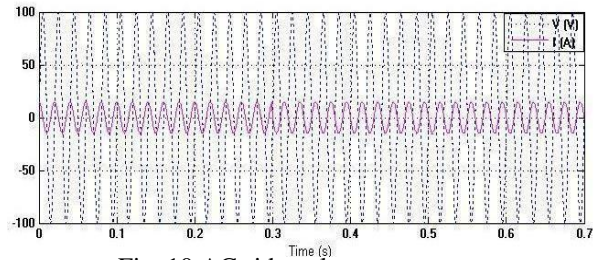


Fig. 10 AC side voltage versus current

Fig. 11 shows the voltage of the battery. The total power generated is greater than the total load before 0.3 s and less than the total load after 0.3 s. Fig. 11 shows that the voltage drops at 0.3 s and recovers to 400V quickly.

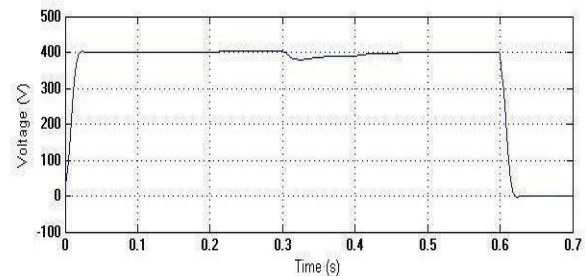


Fig. 11 DC bus voltage transient response in isolated mode.

When the system is at off-MPPT mode in C, with maximum power injection into the battery the dc bus voltage is maintained stable by the boost converter and ac bus voltage is provided by the main converter. Fig. 12, Fig. 13, Fig. 14 shows the dc bus voltage, PV output power, and battery charging current respectively when the dc load decreases from 20 kW to 10 kW at 0.2 s with a constant solar irradiation level 1000W/m

Fig.12shows that the DC bus voltage suddenly drops at 0.6 s and quickly recovers back to 400 V. At 0.6 s the output voltage of the PV system becomes zero and the load acts on the fuel cell. Hence the voltage suddenly drops at 0.6 s.

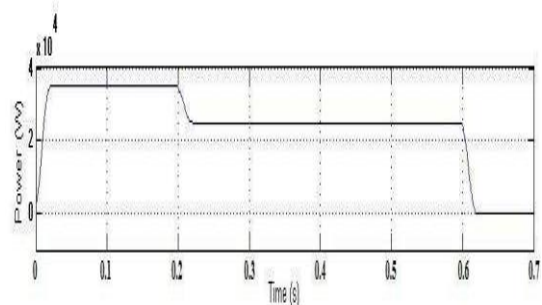


Fig. 12 DC bus voltage

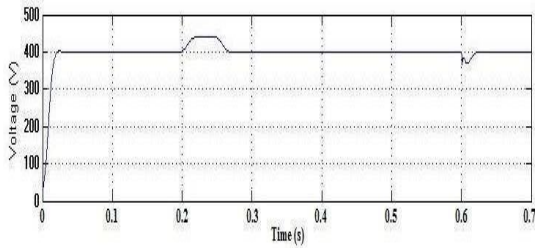


Fig. 13 PV output power

Fig.13 shows that the PV power output drops from the maximum value after 0.2 s, which means that the operating modes are changed from MPPT to off-MPPT mode. The PV output power changes from 35 kW to 25 kW after 0.2s and it decreases linearly from 0.6 s and becomes zero, since the irradiation becomes zero at this instant.

Fig.14 shows the AC side voltage and current of the main converter with variable solar irradiation level and constant dc load. by comparing this characteristics with the characteristics of FLC used system. We can observe that, the reliability of the system is increases.

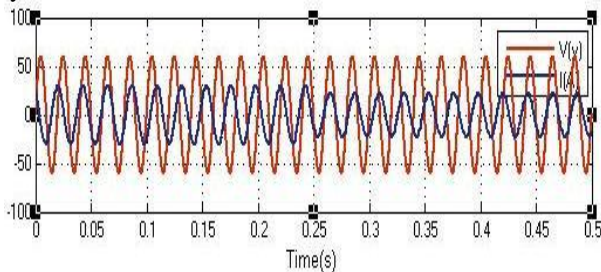


Fig. 6. AC side voltage and current of the main converter with variable solar irradiation level and constant dc load.(with PI controller)

### CONCLUSION

A hybrid ac/dc microgrid is proposed and comprehensively studied in this paper. The models and coordination control schemes are proposed for the all the converters to maintain stable system operation under various load and resource conditions. The coordinated control strategies are verified with Matlab/Simulink. In the proposed system control methods have been incorporated to harness the maximum power from dc and ac sources and to coordinate the power exchange between dc and ac grid. Different resource conditions and load capacities are tested to validate the control methods. The simulation results show that the hybrid grid can operate stably in the grid-tied or isolated mode. But PI controllers are not a reliable controller compared to fuzzy logic controller. This is proved by comparing the output response of these systems.

Although the hybrid grid can reduce the processes of dc/ac and ac/dc conversions in an individual ac or dc grid, there are many practical problems for implementing the hybrid grid based on the current ac dominated infrastructure. The total system efficiency depends on the reduction of conversion losses and the increase for an extra dc link. By using fuzzy logic controller we can reduce those conversion losses. It is also difficult for companies to redesign their home and office products without the embedded ac/dc rectifiers although it is theoretically possible. Therefore, the hybrid grids may be

implemented when some small customers want to install their own PV systems on the roofs and are willing to use LED lighting systems and EV charging systems. The hybrid grid may also be feasible for some small isolated industrial plants with both PV system and wind turbine generator as the major power supply.

### REFERENCES

- [1] Xiong Liu, Peng Wang, and Poh Chiang Loh, "A Hybrid AC/DC Microgrid and Its Coordination Control" IEEE Trans. on SmartGrid, vol. 2, no. 2, pp. 278 - 286 June 2011.
- [2] C. K. Sao and P. W. Lehn, "Control and power management of converter fed MicroGrids," IEEE Trans. Power Syst., vol. 23, no. 3, pp.1088–1098, Aug. 2008.
- [3] M. E. Baran and N. R. Mahajan, "DC distribution for industrial systems: Opportunities and challenges," IEEE Trans. Ind. Appl., vol. 39, no. 6, pp. 1596–1601, Nov. 2003.
- [4] Sannino, G. Postiglione, and M. H. J. Bollen, "Feasibility of a DC network for commercial facilities," IEEE Trans. Ind. Appl., vol. 39, no. 5, pp. 1409–1507, Sep. 2003.
- [5] D. Salomonsson and A. Sannino, "Low- voltage DC distribution system for commercial power systems with sensitive electronic loads," IEEE Trans. Power Del., vol. 22, no. 3, pp.1620–1627, Jul. 2007.
- [6] M. E. Ropp and S. Gonzalez, "Development of a MATLAB/simulink model of a single-phase grid-connected photovoltaic system," IEEE Trans. Energy Conv., vol. 24, no. 1, pp. 195-202, Mar. 2009.
- [7] K. H. Chao, C. J. Li, and S. H. Ho, "Modeling and fault simulation of photovoltaic generation systems using circuit-based model," in Proc. IEEE Int. Conf. Sustainable Energy Technol., Nov. 2008, pp. 290–294.
- [8] D. W. Zhi and L. Xu, "Direct power control of DFIG with constant switching frequency and improved transient performance," IEEE Trans. Energy Conv., vol. 22, no. 1, pp. 110–118, Mar.2007.
- [9] L. Bo and M. Shahidehpour, "Short-term scheduling of battery in a grid-connected PV/battery system," IEEE Trans. Power Syst., vol. 20, no. 2, pp. 1053–1061, May 2005.
- [10] S. A. Daniel and N. AmmasaiGounden, "A novel hybrid isolated generating system based on PV fed inverter-assisted wind-driven induction generators," IEEE Trans. Energy Conv., vol. 19, no. 2, pp. 416–422, Jun. 2004.
- [11] C. Wang and M. H. Nehrir, "Power management of a stand-alone wind/ photovoltaic/fuel cell energy system," IEEE Trans. Energy Conv., vol. 23, no. 3, pp.957– 967, Sep. 2008.
- [13] L. Jong-Lick and C. Chin-Hua, "Small- signal modeling and control of ZVT-PWM boost converters," IEEE Trans. Power Electron., vol.18, no. 1, pp. 2–10, Jan. 2008.